

# Evolution in multiple interactions: a first step beyond the 'double DGLAP' approximation

Jochen Bartels

Universität Hamburg, Germany

DOI: <http://dx.doi.org/10.3204/DESY-PROC-2012-03/19>

We discuss, for the evolution of double-parton densities, a first step beyond the double DGLAP approximation.

## 1 Introduction

In recent years multiple interactions have received increasing interest, both for event generators and for precision calculations of inclusive cross sections[2, 3, 4, 5, 6, 7, 8, 9]. As an example, the double inclusive cross section in the standard collinear approximation

$$d\sigma = \sum_{i_1 i_2} \int dx_1 dx_2 f_{i_1}(x_1, \mu) d\hat{\sigma}_{i_1 i_2 \rightarrow 2 jet}(x_1, x_2, \mu; \mathbf{p}_1, Y_1, \mathbf{p}_2, Y_2) f_{i_2}(x_2, \mu) \quad (1)$$

receives corrections from the two chain configuration (see fig.1, left):

$$d\sigma^{DP} = \frac{m}{\sigma_{eff}} \sum_{i_1, j_1, i_2, j_2} \int dx_1 dy_1 dx_2 dy_2 H_{i_1 j_1}(x_1, y_1, \mu_a, \mu_b) d\hat{\sigma}_{i_1 i_2 \rightarrow jet}(x_1, y_1, \mu_a; \mathbf{p}_1, Y_1) d\hat{\sigma}_{j_1 j_2 \rightarrow jet}(y_2, y_2, \mu_b; \mathbf{p}_2, Y_2) H_{i_2 j_2}(x_2, y_2, \mu_a, \mu_b) \quad (2)$$

In a popular approximation the double parton density is the product of two single parton densities (double DGLAP approximation):

$$H_{ij}(x, y, \mu_a \mu_b) = f_i(x, \mu_a) f_j(y, \mu_b) \quad (3)$$

where each parton density obeys the standard DGLAP evolution equations. On general grounds, however, one expects the evolution of multiparton densities to be more complicated: there should be correlations between the two densities and there are transitions between parton states with different parton numbers. In this contribution we want to make a few comments on aspects of multiparton evolution which go beyond this 'double DGLAP' approximation.

## 2 General aspects of evolution equations

In the context of deep inelastic electron proton scattering and HERA measurements it has become clear that evolution equations can be formulated either in terms of the momentum scale (DGLAP) or in rapidity (BFKL). In the former case, evolution equations can be classified

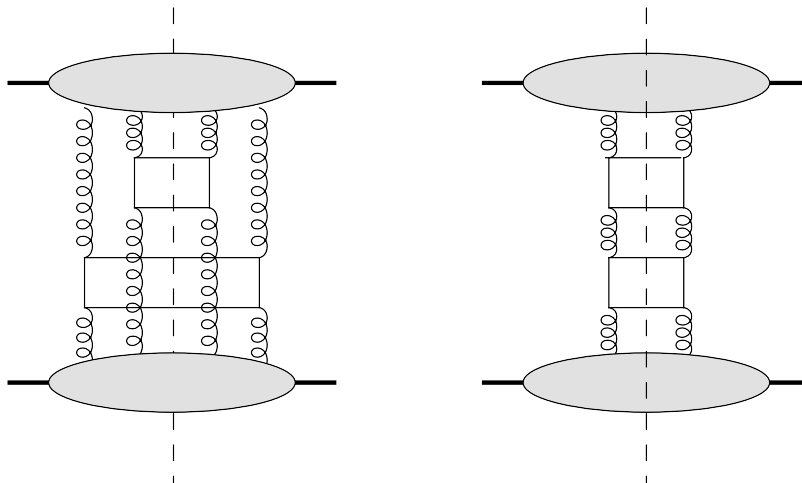


Figure 1: illustration of double and single chain cross sections.

in powers of  $1/Q^2$  (twist): the DGLAP evolution equations belong to the leading twist, and they determine the scale dependence of (single) parton densities. Splitting functions are now known in NLO accuracy. Higher twist evolution equations, in the context of deep inelastic scattering, have been formulated and investigated in [10]. As an example, twist 4 introduces  $t$ -channels with four gluons, and their evolution shares many features with double parton densities. In leading order, the evolution of  $n$ -gluon states is described by the sum over pairwise  $2 \rightarrow 2$  interactions, the nonforward DGLAP splitting functions. Mixing between different twist 4 operators leads to transitions from two to four-parton states. In NLO, the evolution equations will contain also three body interactions. Evolution in rapidity, on the other hand, starts from the BFKL evolution equations and describes BFKL Green's functions of reggeized gluons (sometimes also referred to as unintegrated small- $x$ -gluon densities). Their evolution kernels (presently known in NLO accuracy) are different from the DGLAP kernels, but there exists a common region of validity. The generalization of the BFKL equation to multi-gluon Green's functions (known as the BKP equations [12]) is the analogue of the higher twist evolution, and the evolution, in leading order, is given by the sum of pairwise two-body interactions, described by the nonforward BFKL kernels. Transitions between different gluon states are described by momentum dependent transition kernels, e.g. the  $2 \rightarrow 4$  transition vertex (triple Pomeron vertex). We illustrate the situation in Fig.2.

As mentioned before, the notion of higher twist has been introduced and discussed mainly in the context of deep inelastic scattering where the twist expansion is a power series expansion in  $1/Q^2$ . When searching for an analogous power suppression of a double parton cross section where the large momentum scale is set, for example, by the transverse momenta of the produced jets such a power counting has to be applied with care: there exist regions of momenta where the contributions from double parton scattering are of the same order as those due to single parton scattering; it is only after the integration of the outgoing momenta where a higher twist suppression holds. In contrast to the single parton density cross section no factorization theorem exists for the double scattering formula.

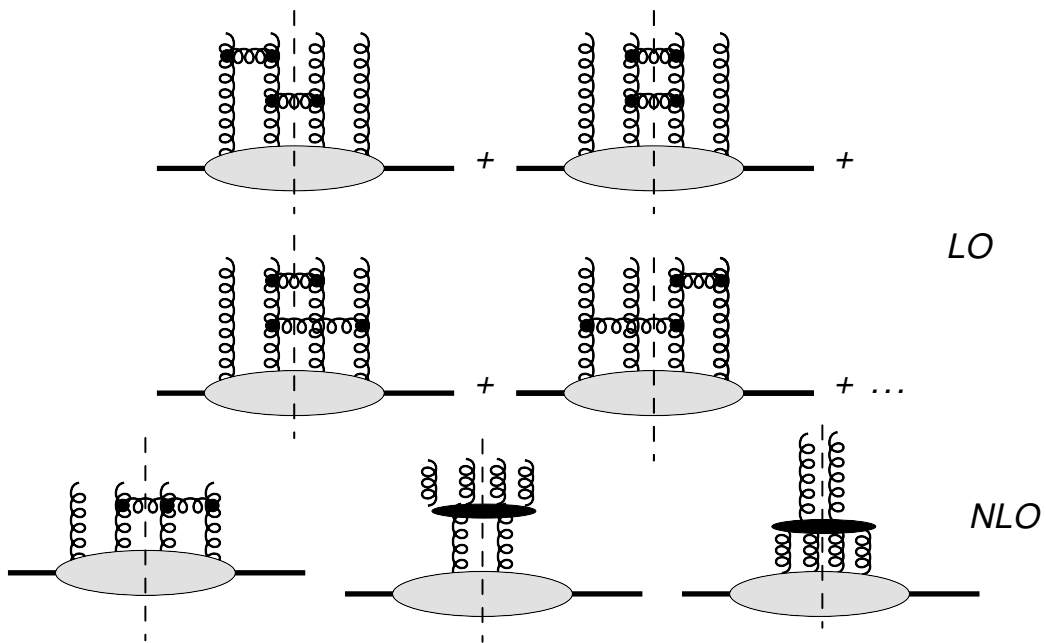


Figure 2: Building blocks of the evolution of double parton densities. The diagrams illustrate both the higher twist evolution and rapidity evolution.

From studies of deep inelastic scattering we know that, at small  $x$ , the rapidity evolution starts to compete with the momentum scale evolution equations. Furthermore, the logarithms in  $1/x$  start to compensate the higher twist suppression (multi-ladder exchanges), and the twist-expansion in powers  $1/Q^2$  becomes useless. The same small- $x$  enhancement is at work also in the double parton cross section: this is why rapidity evolution (BFKL and BKP evolution equations) become increasingly important. This framework also allows to address the question of (soft) rescattering corrections to the double parton formula: from the AGK[11] rules we know that exchanges across the production vertices cancel, not only for single inclusive cross sections but also for double (and higher) inclusive cross sections. A prerequisite for the AGK rules to be valid is the symmetry of the coupling of the four gluons to the proton (Fig.2): this coupling has to be invariant under the exchange of gluons lines (color and momenta), and independent of the position of the cutting line.

### 3 Recombination effects in the two-chain evolution

As we have already indicated (and illustrated in Fig.2), the evolution of double parton densities contains the sum over pairwise  $2 \rightarrow 2$  interactions (ignoring, for the moment, transitions from two to four gluon states). In the factorization approximation ('double DGLAP'), when viewed from the  $t$ -channel, two color singlet ladders are formed, and each ladder, evaluated at zero momentum transfer (Fig.3a) obeys the standard DGLAP evolution equation. This approximation can be justified: the color singlet two gluon system has, at least at small  $x$ , the largest anomalous dimension, and from the initial condition at the proton, there is a strong damping which suppresses large momentum transfer across the ladder. Nevertheless, it is an approximation, and there are corrections to it.

In the following we will consider a special set of corrections which we name 'recombinations'. Counting powers of the strong coupling and powers of large logarithms, this is the first correction to the double DGLAP approximation. A pair of such recombinations is illustrated in Fig.3b: starting from the lower proton we have, initially, two separate ladders, formed by gluons '1' and '4' and by gluons '2' and '3'. After a few steps, there is a recombinations of gluons: gluon '1' goes with gluon '3', and gluon '2' with gluon '4'. The first rungs after this rearrangement define the 'recombination vertex'. It is important to note that, in the double logarithmic approximation (leading power in  $\ln 1/x$  and  $\ln k_{\perp}^2$ ), this recombination is of the same order as the two independent ladders in Fig.3a, i.e. the recombination does not lose any logarithm. There is, however, a color suppression factor of the form

$$\frac{1}{N^2 - 1} \tag{4}$$

In order to become a non-negligible effect, this recombination requires a subtle interplay of momentum and rapidity dependence.

In the following we will give a brief sketch of the argument.

For the further analysis it is important to keep in mind that there are three transverse loop momenta (in Fig. 3c denoted by  $\mathbf{l}'$ ,  $\mathbf{q}$ , and  $\mathbf{l}$ ). Beginning with the analysis of transverse momentum integrals, one looks for configurations where transverse momenta are strongly ordered, both above and below the two production vertices. Smallest momenta are near the proton, largest near the production vertices. A straightforward analysis leads to the observation that the dependence on the loop momentum  $\mathbf{q}$  resides near the two recombination vertices above

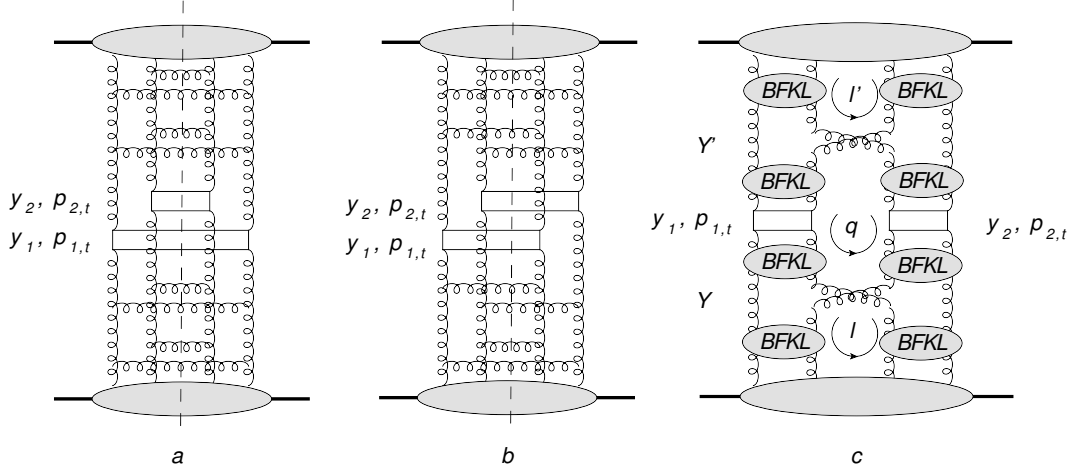


Figure 3: (a) double DGLAP evolution, (b) two recombinations, (c) and a schematic redrawing of the recombination in (b): rungs in (b) are replaced by BFKL amplitudes.

and below the production vertices, and its integral diverges in the infrared region:

$$\int \frac{d^2 q}{(q^2)^2}. \quad (5)$$

As a result, the dominant values are small, the transverse logarithms of the ladders between the recombination vertices and the protons are destroyed, and the recombination vertices become parts of the nonperturbative protons. The situation changes if we allow for small values of  $x$  and include into our analysis the rapidity dependence of the ladders. For this it is convenient to replace the rungs in Fig.3b by BFKL amplitudes, as shown in Fig.3c. The main observation is that, once rapidity intervals may become large, sizable anomalous dimensions will affect the momentum integrals, in particular the integration over  $q$ . The analysis starts from the expression of Fig.3c:

$$\begin{aligned} \frac{d\sigma}{dY_1 dY_2 d^2 p_1 d^2 p_2} &\sim \frac{1}{R_c^2} \frac{1}{R_c^2} \frac{1}{(p_1^2)^2} \frac{1}{(p_2^2)^2} \int \frac{d\mu'}{2\pi i} \int \frac{d\mu}{2\pi i} \int \frac{d\mu'_1}{2\pi i} \int \frac{d\mu_1}{2\pi i} \int \frac{d\mu'_2}{2\pi i} \int \frac{d\mu_2}{2\pi i} \\ &\int dY \int dY' \int \frac{d^2 q}{q^4} \left[ \left( \frac{q^2}{Q_0^2} \right)^{\mu'} e^{(Y_{tot}-Y')\chi(\mu')} \right]^2 \\ &\left[ \left( \frac{p_1^2}{q^2} \right)^{\mu'_1} e^{(Y'-Y_1)\chi(\mu'_1)} \right] \left[ \left( \frac{p_1^2}{q^2} \right)^{\mu_1} e^{(Y_1-Y)\chi(\mu_1)} \right] \left[ \left( \frac{p_2^2}{q^2} \right)^{\mu'_2} e^{(Y'-Y_2)\chi(\mu'_2)} \right] \left[ \left( \frac{p_2^2}{q^2} \right)^{\mu_2} e^{(Y_2-Y)\chi(\mu_2)} \right] \\ &\cdot \left[ \left( \frac{q^2}{Q_0^2} \right)^{\mu} e^{Y\chi(\mu)} \right]^2. \end{aligned} \quad (6)$$

Here  $Y_{tot}$  denotes the total rapidity, and  $Y'$  and  $Y$  are the rapidities of the recombination vertices above and below the production vertices, resp.. For an analysis of this formula one

searches for saddle points of the integrations. Details are described in [1] and in this contribution we only discuss a few results.

An interesting possibility is to put the recombination vertices, in rapidity, as close as possible to the high  $E_T$  dijet production matrix elements. In this case there is no BFKL or DGLAP evolution in the intervals between the produced pairs of jets and the recombination vertices. That is, in the centre of Fig.3, we simply delete the four 'BFKL blobs' nearest to the produced jet pairs. Correspondingly, in (6) we eliminate the third line, together with the integrations over  $\mu_1, \mu_2, \mu'_1, \mu'_2$ . The rapidities  $Y, Y'$  are close to  $Y_i$ , and the  $q^2$  integral takes the form

$$\int \frac{d \ln q^2}{q^2} q^{4(\mu_s + \mu'_s)}, \quad (7)$$

where the saddle point values,  $\mu_s$  and  $\mu'_s$ , follow from the conditions:

$$0 = \chi'(\mu_s)Y + \ln \frac{q^2}{Q_0^2} \quad (8)$$

and

$$0 = \chi'(\mu'_s)(Y_{tot} - Y') + \ln \frac{q^2}{Q_0^2}. \quad (9)$$

Their approximate values are:

$$\mu_s \approx \frac{1}{2} - \frac{1}{\chi''(\frac{1}{2})} \frac{\ln \frac{q^2}{Q_0^2}}{Y}, \quad (10)$$

i.e. the integral over  $q^2$  receives its main contribution from  $q^2$  close to  $\min\{p_1^2, p_2^2\}$ .

Let us consider also a more realistic situation with  $Y_1 = Y_2$  but  $p_2 < p_1$ . Recall that the true argument of the BFKL amplitude is not rapidity but the momentum fraction  $x$ , that is actually we have to write  $\ln(1/x_i)$  instead of  $Y_i$ . When  $p_2 \ll p_1$  for the same rapidities  $Y_1 = Y_2$  we find, in the right ladder, the momentum fraction  $x_2 \sim 2p_2/\sqrt{s} \ll x_1 \sim 2p_1/\sqrt{s}$ . In other words, in this configuration we may put, in Fig.3c, the recombination vertex just into the cell nearest to the left dijet. But then there will be a large  $\ln x$  (and may be  $\ln q^2$ ) interval for the evolution of the right ladders (between the dijets on the rhs and the two recombination vertices). In other words in Fig.3c. we delete only the two 'BFKL blobs' on the lhs below and above the dijet production. Assuming that, in (6), the total rapidity interval  $Y_{tot}$  is very large, we may perform first the rapidity integral

$$\int dY \exp[-Y(\chi(\mu_2) - 2\chi(\mu))] = \frac{1}{\chi(\mu_2) - 2\chi(\mu)} \quad (11)$$

where for the BFKL blobs on the lhs we have set  $\chi(\mu_1) = 0$ , and for  $\mu$  we put its asymptotic value  $\mu = 1/2$ . Now we close the contour of the  $\mu_2$  integration around the pole  $\chi(\mu_2) - 2\chi(\mu) = 0$ : this leads to  $\mu_2 \simeq 0.18$ . The same result is obtained for  $\mu'_2$ . Finally, the  $q^2$  integral takes the form

$$\int^{p_2^2} d \ln q^2 q^{2(1-\mu_2-\mu'_2)}, \quad (12)$$

and the major contribution comes from the domain close to upper limit  $q^2 \sim p_2^2$ .

A closer look reveals still another detail. In the region of interest, for example in a 14 TeV  $pp$ -collision at the LHC, we observe in the central region the dijet with  $p_1 \sim 20\text{GeV}$ , corresponding to  $x \sim 2p_1/\sqrt{s} \sim 0.003$ . For such  $x$ -values, the anomalous dimension observed at HERA is not so large. For  $x < 0.01$  the behaviour of the structure function  $F_2(x, q^2)$  can be parametrized as

$$F_2 = c(q^2)x^{-\lambda} \quad (13)$$

with  $c(q^2) \simeq \text{const}$  and  $\lambda = (0.048 \pm 0.004) \cdot \ln Q^2/\Lambda^2$  [16]. This means that the effective anomalous dimension  $\mu_{eff} = \lambda \ln(1/x) \sim 0.28$  for  $x = 3 \cdot 10^{-3}$ . This value is still large enough to provide the convergence of the  $q^2$  integral (7) in the large  $q^2$  domain for the case considered above where both recombination vertices are just near the dijet production cell. However it is not evident that the parametrization (13) reflects the behaviour of a *single* ladder. At not large  $q^2$  the experimentally measured  $F_2$  already includes some absorptive effects which reduce the growth of  $F_2$  with  $x$  decreasing and thus leads to a lower value of  $\lambda$  in comparison with a single ladder contribution. In other words the true value of  $\mu_{eff}$  which corresponds to a single ladder may be even larger, pushing the characteristic values of  $q^2$  closer to the (lower) hard scale  $p_2^2$ .

## 4 Generalizations

So far we have discussed the effect of two recombinations inside a two-chain contribution: one recombination on each side of the produced jet pairs. Let us first comment on the case where we have no second recombination vertex above the jet pairs: as far as only one recombination vertex is concerned, the integration over  $\mathbf{q}$  is logarithmic. However,  $\mathbf{q}$  runs also through both upper ladders and defines the low momentum scale  $Q_0^2$  where the evolution starts: a large value of  $\mathbf{q}$  therefore kills the evolution in the upper ladders, whereas a low value prevents the evolution in the lower ladders. Therefore, a single recombination vertex is suppressed.

Next a comment on the color suppression factor (4). This suppression applies to the case when, as illustrated in Fig.2, there is evolution above and below the recombination vertex. As we have discussed before, in a preferred situation we have little or no evolution between the recombination vertices and the dijet production vertices. In this case there is no need to reconnect, between the two recombination vertices, the four t-channel gluon lines to color singlet pairs. As result, the color suppression becomes much weaker.

Next we mention another important possibility. Besides the recombination illustrated in Fig.3 there exists another configuration to which our discussion applies. We show this in Fig.4. Below the lower (or above the upper) recombination vertex, color singlet gluon ladders to the right and to the left of the cutting line allow for final states with rapidity gaps. Such configurations are absent in the double DGLAP approximation. Applying our previous discussion, we conclude that the momentum scale at the upper end of the lower rapidity gap,  $q^2$ , will be above  $Q_0^2$  but not too close to the jet momenta  $p_1^2 = p_2^2$ : this allows for 'semihard' diffraction and is in qualitative agreement with inclusive diffraction seen at HERA.

Finally we consider the case of more than two chains, say three chains with three produced pairs of jets. In this case a pair of two recombination vertices can be attributed to any pair of chains, i.e. we have three possibilities. Similarly, for  $n$  chains we have  $\frac{n(n-1)}{2}$  possibilities: these counting factors can easily overcome the color suppression factor in (4). As an example, for  $n = 4$ , the overall counting factor is already  $3/4$ , and it exceeds unity for  $n \geq 5$ . This counting

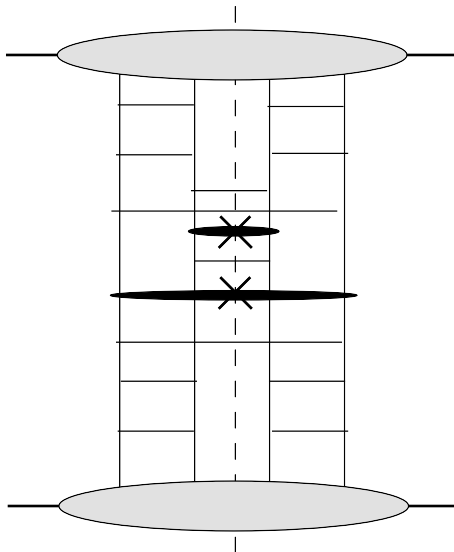


Figure 4: A recombination of two ladders which allows for diffractive states

argument is particularly important for event generators where the number of participating chains may become quite sizable.

The recombination considered in this contribution is very closely related to a recent explanation [13, 14] of the ridge effect observed in  $pp$  collisions at the LHC [15].

## 5 Conclusions

We view this analysis only as first step of investigating the evolution of double parton densities beyond the factorizing approximation. Clearly our analysis has to be made quantitative. Also, it is necessary to go beyond the double leading-log approximation. Work along these lines is in progress.

## References

- [1] J. Bartels and M. G. Ryskin, arXiv:1105.1638 [hep-ph].
- [2] D. Treleani, Phys. Rev. D **76** (2007) 076006 [arXiv:0708.2603 [hep-ph]].
- [3] E. L. Berger, C. B. Jackson and G. Shaughnessy, Phys. Rev. D **81** (2010) 014014 [arXiv:0911.5348 [hep-ph]].
- [4] J. R. Gaunt and W. J. Stirling, JHEP **1003** (2010) 005 [arXiv:0910.4347 [hep-ph]].
- [5] J. R. Gaunt, C. H. Kom, A. Kulesza and W. J. Stirling, Eur. Phys. J. C **69** (2010) 53 [arXiv:1003.3953 [hep-ph]].
- [6] M. Strikman and W. Vogelsang, Phys. Rev. D **83** (2011) 034029 [arXiv:1009.6123 [hep-ph]].
- [7] M. Diehl and A. Schafer, Phys. Lett. B **698** (2011) 389 [arXiv:1102.3081 [hep-ph]].
- [8] C. Flensburg, G. Gustafson, L. Lonnblad and A. Ster, arXiv:1103.4320 [hep-ph].
- [9] M. G. Ryskin and A. M. Snigirev, arXiv:1103.3495 [hep-ph].

- [10] A. P. Bukhvostov, G. V. Frolov, L. N. Lipatov and E. A. Kuraev, Nucl. Phys. B **258** (1985) 601.
- [11] V. A. Abramovsky, V. N. Gribov and O. V. Kancheli, Yad. Fiz. **18** (1973) 595 [Sov. J. Nucl. Phys. **18**; M. Salvadore, J. Bartels and G. P. Vacca, arXiv:0709.3062 [hep-ph].
- [12] J. Bartels, Nucl. Phys. **B175** (1980) 365.  
J. Kwiecinski, M. Praszalowicz, Phys. Lett. **B94** (1980) 413.  
T. Jaroszewicz, Acta Phys. Polon. **B11** (1980) 965.
- [13] A. Dumitru, K. Dusling, F. Gelis, J. Jalilian-Marian, T. Lappi, R. Venugopalan, Phys. Lett. **B697** (2011) 21-25. [arXiv:1009.5295 [hep-ph]].
- [14] K. Dusling and R. Venugopalan, arXiv:1201.2658 [hep-ph].
- [15] V. Khachatryan *et al.* [CMS Collaboration], JHEP **1009** (2010) 091. [arXiv:1009.4122 [hep-ex]].
- [16] C. Adloff *et al.* [ H1 collaboration ], Phys. Lett. **B520** (2001) 183.